Design and Simulation of Full State Feedback Controller for DC Motor

K. Love[*], C. Kriger, T. Nomzamo

Department of Electrical, Electronics and Computer Engineering, Faculty of Engineering and the Built Environment, Cape Peninsula University of Technology, Cape Town, South Africa
[*]corresponding author's email: kevinluffylove@gmail.com

Abstract – *This paper presents the design and simulation of a Full State Feedback (FSFB) controller which controls the angular position of Direct Current (DC) motor. The controller is used to reduce the rise time of the system when given a position set point. An integral controller is then added to reduce the steady state error of the output. Once the transfer function of the DC motor is found, the mathematical model is converted to state space. The process involves utilizing the Pole placement technique to identify the state feedback gain, which subsequently improves the system's response time. The results, which are simulated in Simulink, show that the addition of FSFB control significantly reduces the rise time of the response from 4.013s to 0.966s. To overcome the steady-state error of 9.84, integral control is added which reduced the error to zero. A reduction in rise time and steady state-error proves that a FSFB controller with integral control performs better than the original closed loop system without a controller. The research contribution is based on the mathematical modeling of a DC motor and the development of a state feedback controller, aiming to simplify the modeling process with its associated controllers. The methods presented can be used on any DC motor with known parameters. Finally, the control system is tested using random set points to prove the resilience of the controller to input changes.*

Keywords: *DC motor, full state feedback controller, MATLAB Simulink, state space*

I. Introduction

Direct Current (DC) Motors are often used in industrial applications because of their simplicity, reliability, convenience across a range of applications and their cost effectiveness [1]. The motors are normally used with gears to provide a higher torque output from the motor shaft to the output of the gearbox. The high torque provided is one of the main reasons why DC motors are preferred over other motors [2]. Another advantage of DC motors is the fast response times to rotational changes as the motor can operate at high speeds [3]. High torque and fast response times are important factors needed for positional control of DC motors in various technological and industrial applications that require precision and stability.

Position control of a DC motor is possible by using an instrument such as an encoder to feed the angular position and angular speed back into the system to create closed-loop control [4]. Other instruments can also be used as demonstrated in [5] where the position of DC motors in a robot gripper is determined using strain gauge feedback. Although this method is more cost effective, encoder feedback is still the most reliable for position feedback.

Actuating a DC motor to change its position will cause the motor to reach the desired set point over time, depending on the motor dynamics. There is no control over the response of the DC motor and therefore a controller is developed and added to change the response.

Different types of controllers have been proposed by researchers to control a DC motor. In [1] and [3] the conventional Proportional-Integral-Derivative (PID) control method is used, with the encoder feedback serving as the process variable, and a potentiometer as the set point. The results show that the addition of a controller improved the set point tracking and robustness of the system when trying to achieve a desired angular position of a DC motor.

Many other PID controllers have been developed for DC motor position control and are found in [6]-[13]. All the authors are successful in decreasing settling times and increasing rise times but had to go through trial-and-error methods to figure out the proportional, integral, and derivative gains required for PID control which is time consuming. While PID is still the most common controller

for DC motor position control, other authors have used different approaches to achieve better system responses and prevent guessing of gain values.

Reference [2] utilized a hybrid controller combining both PID and Linear Quadratic Regulator (LQR) control to minimize the deviation from the desired set point. The controller's performance achieved zero percent overshoot with a reduction in rise time which met the objectives of the design approach. In [14] an optimal nonlinear PID controller is used to control the position. Comparative testing against a non-optimized PID controller showed that the optimized controller demonstrated advanced tracking performance, compared to the conventional PID control, when trying to achieve the desired time performance specifications.

Robust controller design is presented in [15] where H∞ and H2 methods are used for stabilizing a DC motor system that has uncertainties such as motor dynamics and external perturbation. Uncertainties with real time systems are explored in [16] by using a fuzzy logic controller to implement position control on real-time operating system.

In references [4], [16]-[21]. Modern control theory is applied by creating FSFB controllers through the utilization of state space analysis and pole placement technique. FSFB controllers use the system's state variables, such as velocity and angular position, to solve for a gain matrix K that is used to change the response of a system. The pole placement technique is used by the authors to determine the desired response of the system based on characteristics such as the system overshoot and settling time.

Reference [4] compared the full state feedback controller response to a PID controller with the same step input. The FSFB controller had better set point tracking, showing faster system rise, and settling times. Reference [17] concluded that the more negative the poles are placed in the s-plane, when using the pole placement technique, the faster the rise and settling times of the system will be.

Reference [19] compared the responses of three different controllers using the MATLAB/Simulink programming environment. The authors compared FSFB, FSFB with feed forward gain and FSFB with integral controller. The results showed that the response and stability of the full state feedback with integral controller was the best when tested with a unit step input. The author did not test the full capacity of the controller by simulating higher set points or drastic change in position set point values.

Reference [16] went a step further by adding a Luenberger observer to the FSFB controller to estimate states that are not measurable. The observer also reduces the number of sensors needed as certain states can be estimated and fed back into the system. The author also proved that the estimated and actual measured values are similar when simulating and implementing the system.

This paper presents the design and simulation results of an FSFB controller with integral control to control the angular position of a DC motor. FSFB control is chosen over PID control as the response times and robustness of the controller has been proven to be better. An observer is not considered as all states are simulated and will not need to be measured.

Firstly, the mathematical model of the DC motor for the open loop and closed loop systems are derived and converted to state space form using modern control theory. State space form is used as it is less complex and allows for easier design than using differential equations to model systems. The transfer function of the DC motor closed loop system is simplified in a form that makes it easier to convert to state space and develop the model of the system. This is done by substituting new terms into the mathematical model to reduce the complexity of the closed loop transfer function as well as the converted state space equations. Then, the controller is designed for the closed loop system to meet specific requirements such as a reduction in rise time and zero percent overshoot. The open-loop, closed-loop, FSFB controller, and FSFB controller with integral control, are all compared in a case study which tests the system responses and stability through simulation using the MATLAB/Simulink software environment. Each system is subjected to a unit step input and the performance is compared in terms of rise time, settling time, steady-state error, and overshoot.

Previous published work has not fully tested the capabilities of the designed controllers to rapid changes in the position set point. This study uses random input set points to test the robustness of the response of the FSFB controller with integral control when there is a rapid change in the input position set point.

II. Modeling of a DC Motor

In control systems it is advisable to first design and simulate the appropriate model of the plant before applying the controller to the actual hardware. The system model is used to simulate and validate the plants' response to changes in parameters. The DC motor is designed to convert electrical energy to mechanical energy. Therefore, the DC motor, shown in Fig. 1, is modelled by finding the electrical and mechanical system equations and then combining the equations to form the electro-mechanical transfer function, where:

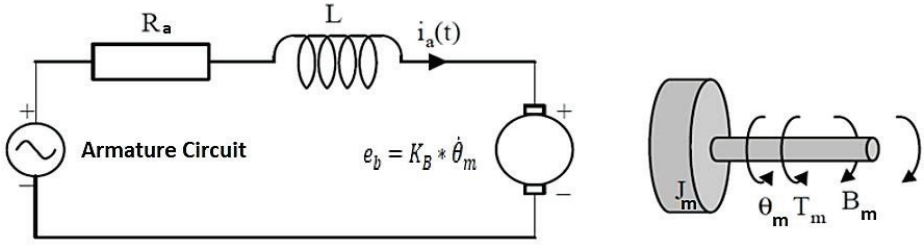|	
V_a	Armature voltage
R_a	Armature resistance
L_a	Armature inductance
i_a	Armature current
e_b	Back electromotive force
K_B	Electromotive force constant
$\dot{\theta}_m$	Angular velocity
θ_m	Angular position
T_m	Input torque
J_m	Moment of inertia
B_m	Damping coefficient
K_T	Torque constant

Fig. 1. Electromechanical diagram of a DC motor

A. Modeling of the Electrical Component of DC Motor

The electrical component of a DC motor is modelled using Kirchhoff's voltage law, which states the sum of potential differences in a closed circuit is equal to zero [17]. The balance equation is defined by

$$V_a(t) - R_a i_a(t) - L_a \frac{di_a}{dt} - e_b = 0 \qquad (1)$$

where V_a is the voltage source, R_a is the resistance of the armature, L_a is the inductance of the armature, e_b is the back electromotive force generated from the load, and $i_a(t)$ is the armature current that flows through the circuit with time. From (1), the voltage is expressed as

$$V_a(t) = R_a i_a(t) + L_a \frac{di_a}{dt} + e_b \qquad (2)$$

e_b in the electrical circuit is expressed as

$$e_b = K_B \dot{\theta}_m \qquad (3)$$

where K_B is the electromotive force constant of the DC motor and $\dot{\theta}_m$ is the angular velocity of the DC motor.

Substituting (3) into (2) yields

$$V_a(t) = R_a i_a(t) + L_a \frac{di_a}{dt} + K_B \dot{\theta}_m \qquad (4)$$

Taking the Laplace transform of (4) obtains

$$V_a(s) = R_a I_a(s) + L_a s I_a(s) + K_B s \theta_m(s) \qquad (5)$$

where θ_m is the angular position of the DC motor, and s i s a complex frequency domain parameter.

Rearranging (5) yields

$$V_a(s) - K_B s \theta_m(s) = I_a(s)(R_a + L_a(s)) \qquad (6)$$

It is necessary to convert all differential equations to the frequency domain using Laplace transformations to allow for easier algebraic manipulation of the time domain equations. The conversion also makes it easier to convert the electrical and mechanical components into one electromechanical mathematical model.

B. Modeling of the mechanical component of a DC motor

It is important to model the mechanical component of the DC motor because the output rotational movement of the shaft is related to the input current from the electrical component. The electrical current flowing through the circuit causes a fixed magnetic field due to the magnet component in the DC motor [22]. This magnetic field applies a force on the inertial mass that causes an input torque which is defined using Newton's 2nd law. The balance equation is defined by:

$$T_m - B_m \dot{\theta}_m = J_m \ddot{\theta}_{mL}. \qquad (7)$$

where T_m is the input torque to the load, B_m is the damping coefficient, $\dot{\theta}_m$ is the angular velocity of the DC motor, $\ddot{\theta}_m$ is the angular acceleration of the DC motor, J_m is the initial moment of inertia.

The initial torque generated is expressed as

$$T_m = K_T * i_a(t) \qquad (8)$$

where K_T is the DC motor torque constant, and $i_a(t)$ is the armature current flows through the circuit with time.

Substituting (8) into (7) yields

$$K_T i_a(t) - B_m \dot{\theta}_m = J_m \ddot{\theta}_m \qquad (9)$$

This substitution is crucial as it allows the like term of $i_a(t)$ to be in both the electrical and mechanical balance equations.

Taking the Laplace transform of (9) yields

$$K_T I_a(s) - s B_m \theta_m(s) = J_m s^2 \theta_m(s) \qquad (10)$$

Rearranging (10) the balance equation of the mechanical component of the DC motor is defined by

$$K_T I_a(s) = s(J_m s + B_m)\theta_m(s) \qquad (11)$$

C. DC Motor open loop transfer function

It is necessary to obtain the complete electromechanical transfer function of a DC motor to simulate the system. The electrical and mechanical component system equations, as described in (6) and (11) respectively, are

combined to formulate the full system. This is done by using the like term of $I_a(s)$ which is found in both equations. Making $I_a(s)$ the subject of each formula for (6) and (11) and then making the two equations equal obtains

$$V_a(s) - K_B s\theta_m(s) = \frac{(L_a s + R_a)(J_m s + B_m)}{K_T} s\theta_m(s) \quad (12)$$

Rearranging (12) yields

$$V_a(s) = \left[\frac{(L_a s + R_a)(J_m s + B_m) + K^2}{K_T}\right] s\theta_m(s) \quad (13)$$

Rearranging (13) to find the transfer function for input acceleration to output voltage obtains

$$\frac{\dot{\theta}_m(s)}{V_a(s)} = \frac{K_B}{(J_m s + B_m)(L_a s + R_a) + K_B * K_T} \quad (14)$$

Positional control is the objective of this work and therefore (14) is integrated to show the relationship between position and voltage. Integrating both sides of (14) obtains

$$\frac{\theta_m(s)}{V_a(s)} = \frac{K_B}{s[(J_m s + B_m)(L_a s + R_a) + K_B * K_T]} \quad (15)$$

Considering armature inductance in a fixed motor as negligible simplifies (15) to obtain

$$\frac{\theta_m(s)}{V_a(s)} = \frac{K_B}{R_a J_m s^2 + s[R_a B_m + K_B * K_T]} \quad (16)$$

Simplifying (16) to find the full electro-mechanical component of the DC motor where voltage is the input and angular position is the output obtains

$$\frac{\theta_m(s)}{V_a(s)} = \frac{\frac{K_B}{R_a}}{J_m s^2 + s[\frac{R_a B_m + K_B * K_T}{R_a}]} \quad (17)$$

To reduce the complexity of the transfer function to allow for easier modeling of the system, new variables K_m and a_m are used where

$$K_m = \frac{K_B}{R_a J_m} \quad (18)$$

and

$$a_m = \frac{R_a B + K_B * K_T}{R_a J_m} \quad (19)$$

Substituting (18) and (19) into (17) yields

$$\frac{\theta_m(s)}{V_a(s)} = \frac{K_m}{s(s + a_m)} \quad (20)$$

The motor parameters shown in Table I are substituted into (20) to obtain the complete transfer function for the specified DC motor. The motor used is a 6000 Revolutions Per Minute (RPM) 12V DC motor with a 1:270 gearbox. The load moment of inertia and damping ratios are from the incremental encoder that is mechanically connected through a 1:1 gear ratio at the end of the motor shaft.

The total moment of inertia is defined as

$$J_m = J_a + J_L \left(\frac{N_1}{N_2}\right)^2 = 0.013 Kg/m^2 \quad (21)$$

where J_a is the moment of inertia of the armature, J_L is the moment of inertia of the load, N_1 is the number of gear

teeth on the motor side of the gearbox, and N_2 is the number of gear teeth on the load side of the gearbox.

The total damping coefficient is defined as

$$B_m = B_a + B_L \left(\frac{N_1}{N_2}\right)^2 = 0.00002 Ns/m \quad (22)$$

where B_a is the motor damping coefficient, and B_L is the load damping coefficient.

TABLE I
DC MOTOR PARAMETERS

Symbol	Parameter	Value
R_a	Armature resistance	14.3 ohm
L_a	Armature inductance	0 henry
K_B	Electromotive force constant	0.425 volt/(rad/sec)
K_T	Torque constant	2.3 N-m/ampere
J_a	Moment of inertia of the armature	0.013 Kg/m²
J_L	Moment of inertia of the load	0.001 Kg/m²
B_a	Motor damping coefficient	0.00001 Ns/m
B_L	Load damping coefficient	1 Ns/m
N_1	Number of gears teeth on motor	1 Tooth
N_2	Number of gears teeth on load	270 Teeth

Substituting the motor parameters from Table I into (18) yields

$$K_m = \frac{0.425}{14.3 * 0.013} = 2.2862 \quad (23)$$

Substituting the motor parameters from Table I into (19) yields

$$a_m = \frac{14.3 * 0.00002 + (0.425 * 2.3)}{14.3 * 0.013} = 5.26 \quad (24)$$

Substituting the values for K_m and a_m into (20) yields

$$\frac{\theta(s)}{V_a(s)} = \frac{5,26}{s(s + 2.2862)} \quad (25)$$

(25) is the transfer function for the open loop DC motor control system used in the simulation model.

III. State Space Model

As the systems become more complex, the task of modeling using differential equations and transfer functions becomes increasingly challenging. Therefore, it is necessary to use the state space representation to allow for easier design and modeling of systems. The state space representation of a physical system consists of a set of inputs, outputs, and state variables in a mathematical model which is related by first-order differential equations [23]. The states which change with time in a DC motor are position, velocity, and armature current. In this work, only position and velocity are considered.

The state space equations of a plant are expressed as

$$\dot{x}(t) = Ax(t) + Bu(t) \tag{26}$$

$$y(t) = Cx(t) + Du(t) \tag{27}$$

where A is the state matrix, B is the input matrix, C is the output matrix, and D is the feedthrough matrix. The A matrix captures the dynamics of the linear system, which includes how the energy of the system is captured, stored, and moved. The B matrix determines how the system responds to the inputs. All four matrices are calculated by finding the derivatives of the states of the system. Rearranging (20) to make angular position the subject of the formula obtains

$$\theta_m(s) = \frac{K_m}{s(s+a_m)} V_a(s) \tag{28}$$

Simplifying (28) yields

$$s^2\theta_m(s) + s\theta_m(s)a_m = K_m V_a(s) \tag{29}$$

Taking the inverse Laplace transform of (29) and making angular acceleration the subject of the formula shows

$$\ddot{\theta}_m = -\dot{\theta}_m a_m + K_m V_a(t) \tag{30}$$

The states of the system are expressed as

$$y = \theta_m = X_1 \tag{31}$$

and

$$\dot{y} = \dot{\theta}_m = \dot{X}_1 = X_2 \tag{32}$$

and

$$\ddot{y} = \ddot{\theta}_m = \ddot{X}_1 = \dot{X}_2 = -\dot{\theta}_m a_m + K_m V_a(t) \tag{33}$$

where X_1 and X_2 are vector components.

These components make it easier to formulate the derivatives of the states. Once all the derivatives are found,

it is possible to find the state space equations by making the derivatives the subject of the formula expressed as

$$\dot{X}_1 = X_2 \tag{34}$$

and

$$\dot{X}_2 = -X_2 a_m + K_m V_a(t) \tag{35}$$

The output equation is expressed as

$$y = X_1 \tag{36}$$

The matrices of the state space model are expressed as

$$A = \begin{bmatrix} 0 & 1 \\ 0 & -a_m \end{bmatrix}, \; B = \begin{bmatrix} 0 \\ K_m \end{bmatrix},$$

$$C = \begin{bmatrix} 1 & 0 \end{bmatrix} \begin{bmatrix} 0 \\ K_m \end{bmatrix}, \; D = 0$$

Finally, the state space model of the open loop plant with no feedback is expressed as

$$\begin{bmatrix} \dot{\theta} \\ \ddot{\theta} \end{bmatrix} = \begin{bmatrix} 0 & 1 \\ 0 & -a_m \end{bmatrix} \begin{bmatrix} \theta \\ \dot{\theta} \end{bmatrix} + \begin{bmatrix} 0 \\ K_m \end{bmatrix} u(t) \tag{37}$$

$$y(t) = \begin{bmatrix} 1 & 0 \end{bmatrix} \begin{bmatrix} 0 \\ K_m \end{bmatrix} \tag{38}$$

Substituting the values calculated for K_m and a_m into (37) and (38) gives the state space model as

$$\begin{bmatrix} \dot{\theta} \\ \ddot{\theta} \end{bmatrix} = \begin{bmatrix} 0 & 1 \\ 0 & -5.26 \end{bmatrix} \begin{bmatrix} \theta \\ \dot{\theta} \end{bmatrix} + \begin{bmatrix} 0 \\ 2.2862 \end{bmatrix} u(t) \tag{39}$$

$$y(t) = \begin{bmatrix} 1 & 0 \end{bmatrix} \begin{bmatrix} 0 \\ 2.2862 \end{bmatrix} \tag{40}$$

Fig. 2 shows the actual Simulink block diagram of the DC motor in a state space form with unity feedback. The addition of the feedback in Fig. 2 creates a difference between the input and the output that allows the controller to actuate the motor towards the set point.
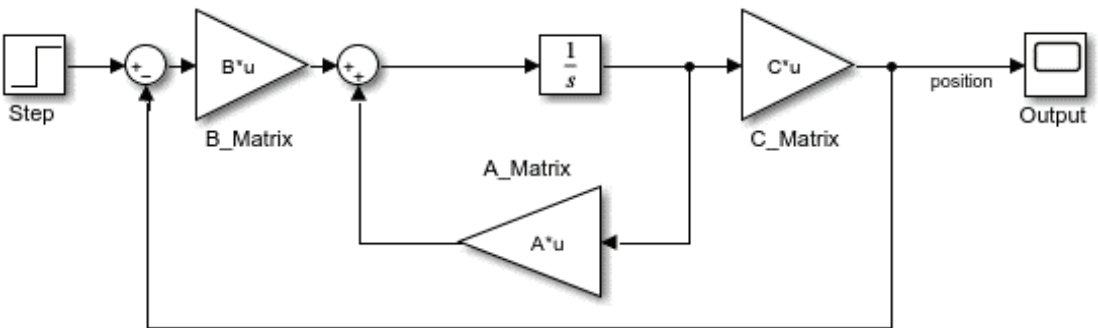

Fig. 2. Simulink block diagram of a state space representation of closed-loop DC motor with a step input

The addition of closed-loop control is done with an encoder or resolver, by subtracting the output of the sensor from the input set point to create a steady state error that allows the system to reach a steady state. A step input is used to test the response of the closed-loop system.

The feedback function in MATLAB is used to add unity feedback to the state space model shown in (39) and (40) to give the closed-loop state space model of the DC motor system as

$$\begin{bmatrix} \dot{\theta} \\ \ddot{\theta} \end{bmatrix} = \begin{bmatrix} -5.26 & -2.2862 \\ 1 & 0 \end{bmatrix} \begin{bmatrix} \theta \\ \dot{\theta} \end{bmatrix} + \begin{bmatrix} 2 \\ 0 \end{bmatrix} u(t) \qquad (41)$$

$$y(t) = \begin{bmatrix} 0 & 1.1431 \end{bmatrix} \begin{bmatrix} \theta \\ \dot{\theta} \end{bmatrix} \qquad (42)$$

IV. State Feedback Controller Design

A. Full State Feedback Controller

An FSFB controller allows the movement of the system poles to any desired location. Moving the poles of a system results in different responses in factors such as rise time, overshoot, frequency, gain, and settling time. Poles are moved from the right-hand plane to the left, causing the system to become stable. This is done by multiplying each state by a certain gain K and feeding the result back into the system.

1. Control law

To determine how a system responds to input signals and regulates its output signals to achieve its desired objective, it is necessary to determine its control law. The control law is a mathematical representation that shows the behavior of a control system. Developing a control law is very beneficial when designing a system, performing optimization, analyzing stability, testing model compatibility, and preventing rework. Determining the control law before designing the control system establishes a solid foundation for the system's overall performance.

The first step is to determine the control law for an FSFB controller. Because the system is considered linear, there are no external disturbance therefore the output of the system is equal to the states. Applying this logic to matrices C and D into (27), (43) is formed.

$$y(t) = x(t) \qquad (43)$$

The control law for an FSFB controller is given by

$$u(t) = -Kx(t) \qquad (44)$$

where K is the gain matrix.

Substituting (44) into (26) yields

$$\dot{x}(t) = Ax(t) + B(-Kx(t)) \qquad (45)$$

Rearranging (45) to find the closed-loop state space representation of the system yields

$$\dot{x}(t) = (A - BK)x(t) \qquad (46)$$

The A matrix in a closed-loop system is defined as

$$A_{CL} = A - BK \qquad (47)$$

where A_{CL} is the closed-loop A matrix.

Substituting (47) into (46) yields

$$\dot{x}(t) = A_{CL} \cdot x(t) \qquad (48)$$

2. Controllability

A DC motor system model needs to be in a controllable state to use an FSFB controller with pole placement. To check controllability, it is necessary to test if the system model is already in controllable canonical form. The test for controllability is expressed as

$$P_C = \begin{bmatrix} A & AB \end{bmatrix} \qquad (49)$$

where P_C is the controllability matrix.

Substituting matrices, A and B into (49) yields

$$P_C = \begin{bmatrix} \begin{bmatrix} -5.26 & -2.2862 \\ 1 & 0 \end{bmatrix} & \begin{bmatrix} -5.26 & -2.2862 \\ 1 & 0 \end{bmatrix}\begin{bmatrix} 2 \\ 0 \end{bmatrix} \end{bmatrix} \qquad (50)$$

Simplifying (50) yields

$$P_C = \begin{bmatrix} 2 & -10.5201 \\ 0 & 2 \end{bmatrix} \qquad (51)$$

As shown in (51), the second row of the matrix P_C is not dependent on the first row and therefore the rank is 2, proving that the system is controllable.

3. Solve for gain matrix K

The value of the gain matrix K is used to move the poles of a system to a desired location. It is necessary to move the poles of the system to decrease the system's rise time. The gain matrix K is multiplied by the input matrix B and then subtracted from the state matrix A. This shows that the value of K has a direct effect on the states of the system.

Before moving the poles to a desired location, it is necessary to find the characteristic equation of the closed loop system with state feedback control. This is done by finding the value of the matrix A_{CL} and then finding the eigenvalues of the closed-loop matrix. The values for matrix A, B, and K are substituted into (45) to obtain

$$A_{CL} = \begin{bmatrix} -5.26 & -2.2862 \\ 1 & 0 \end{bmatrix} - \begin{bmatrix} 2 \\ 0 \end{bmatrix} \begin{bmatrix} K_1 & K_2 \end{bmatrix} \qquad (52)$$

where K_1 and K_2 are vectors of the matrix K.

Simplifying (52) through matrix multiplication obtains

$$A_{CL} = \begin{bmatrix} -5.26 & -2.2862 \\ 1 & 0 \end{bmatrix} - \begin{bmatrix} 2K_1 & 2K_2 \\ 0 & 0 \end{bmatrix} \qquad (53)$$

Simplifying (53) through matrix subtraction obtains

$$A_{CL} = \begin{bmatrix} -5.26 - 2K_1 & -2.2862 - 2K_2 \\ 1 & 0 \end{bmatrix} \qquad (54)$$

The next step is to find the eigenvalues of matrix A_{CL}. The formula used to calculate the eigenvalues of a system is expressed as

$$0 = det(\lambda I - A_{CL}) \qquad (55)$$

where I is a 2x2 identity matrix, and λ is a mathematical constant. Substituting matrix A_{CL} into (55) yields

$$0 = det\left(\begin{bmatrix} \lambda & 0 \\ 0 & \lambda \end{bmatrix} - \begin{bmatrix} -5.26 - 2K_1 & -2.2862 - 2K_2 \\ 1 & 0 \end{bmatrix}\right) \qquad (56)$$

Simplifying (56) yields

$$0 = det\left(\begin{bmatrix} \lambda - (-5.26 - 2K_1) & -(-2.2862 - 2K_2) \\ -1 & \lambda \end{bmatrix}\right) \quad (57)$$

Simplifying (57) yields

$$0 = det\left(\begin{bmatrix} \lambda + 5.26 + 2K_1 & 2.2862 + 2K_2 \\ -1 & \lambda \end{bmatrix}\right) \quad (58)$$

Finding the determinant of (58) obtains

$$0 = (\lambda + 5.26 + 2K_1)\lambda - (-1 * (2.2862 + 2K_2)) \quad (59)$$

Simplifying (59) obtains the characteristic equation of the closed-loop system expressed as

$$0 = \lambda^2 + 5.26\lambda + 2K_1\lambda + 2.2862 + 2K_2 \quad (60)$$

To achieve a faster rise time, the poles -2 and -6 are selected. These poles are known as the desired poles and is expressed as the desired characteristic equation

$$0 = \lambda^2 + 8\lambda + 12 \quad (61)$$

The values for K_1 and K_2 are solved by equating the coefficients of the like terms in the closed loop and desired characteristic (60) and (61). The equated characteristic equations are expressed as

$$5.26 + 2K_1 = 8 \quad (62)$$

and

$$2.2862 + 2K_2 = 12 \quad (63)$$

Substituting the values of K_1 and K_2 into the gain matrix **K** yields

$$K = [K_1 \quad K_2] = [1.37 \quad 4.8569] \quad (64)$$

Substituting the gain matrix **K** back into (52), the closed-loop **A** matrix is expressed as

$$A_{CL} = \begin{bmatrix} -8 & -12 \\ 1 & 0 \end{bmatrix} \quad (65)$$

The state space model of the closed-loop system with an FSFB controller is expressed as

$$\begin{bmatrix} \dot{\theta} \\ \ddot{\theta} \end{bmatrix} = \begin{bmatrix} -8 & -12 \\ 1 & 0 \end{bmatrix} \begin{bmatrix} \theta \\ \dot{\theta} \end{bmatrix} + \begin{bmatrix} 2 \\ 0 \end{bmatrix} u(t) \quad (66)$$

$$y(t) = [0 \quad 1.1431] \begin{bmatrix} \theta \\ \dot{\theta} \end{bmatrix} \quad (67)$$

4. Simulink simulation

Fig. 3 shows the actual Simulink block diagram of the DC motor in state space form controlled by the developed FSFB controller. The gain matrix **K** is multiplied by the states and the output is fed back into the control system to change the response.
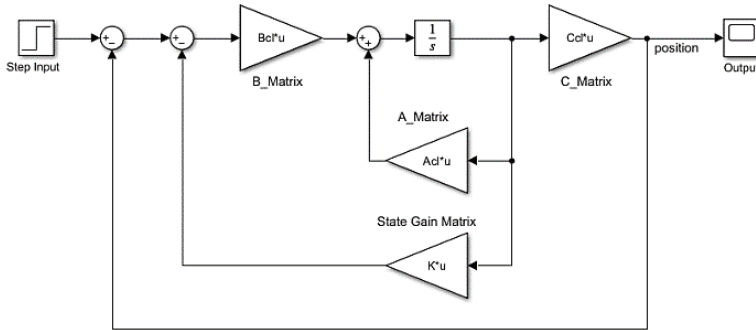

Fig. 3. Simulink block diagram of a step input to a DC motor with an FSFB controller.

B. Integral Control

1. Control law

The control law for integral control is a closed-loop system is expressed as

$$\dot{x}_i = -Cx(t) + r(t) \quad (68)$$

where $r(t)$ is the input to the controller and $\dot{x}_i$ is the input state of the integrator.

The new control law is expressed as

$$u(t) = -Kx(t) + K_i x_i(t) \quad (69)$$

where K_i is the integral gain x_i and is the output state of the integrator. The state space model of the plant with FSFB and integral control according to the new control law is found by substituting (69) into (26) to obtain

$$\dot{x} = Ax(t) + B(-Kx(t) + K_i x_i(t)) \quad (70)$$

Simplifying (70) yields

$$\dot{x} = (A - BK)x(t) + BK_i x_i(t) \quad (71)$$

The state space model of the closed-loop system with an FSFB controller with integral control is expressed as

$$\begin{bmatrix} \dot{x} \\ \dot{x}_n \end{bmatrix} = \begin{bmatrix} A - BK & BK_i \\ -C & 0 \end{bmatrix} \begin{bmatrix} x \\ x_n \end{bmatrix} + \begin{bmatrix} 0 \\ 1 \end{bmatrix} r(t) \tag{72}$$

$$y(t) = \begin{bmatrix} C & 0 \end{bmatrix} \begin{bmatrix} x \\ x_n \end{bmatrix} \tag{73}$$

2. Solve for gains **K** and K_i

It is necessary to find values for **K** and K_i to achieve the desired transient response of the DC motor system. This is done by moving the poles to desired locations. Before moving the poles, the characteristic equation of the closed loop system with FSFB and integral control must be found. This is done by finding the value of A_{CL}, B_{CL}, and C, then substituting these values into the state space model. A_{CL} is expressed as

$$A_{CL} = A - BK = \begin{bmatrix} -5.26 - 2K_1 & -2.286 - 2K_2 \\ -1 & 0 \end{bmatrix} \tag{74}$$

B_{CL} is expressed as

$$B_{CL} = BK_i = \begin{bmatrix} 2 \\ 0 \end{bmatrix} * K_i \tag{75}$$

C is expressed as

$$C = \begin{bmatrix} 0 & 1.1431 \end{bmatrix} \tag{76}$$

Substituting matrices A_{CL}, B_{CL} and C into the state space model (72) and (73) yields

$$\begin{bmatrix} \dot{x}_1 \\ \dot{x}_2 \\ \dot{x}_i \end{bmatrix} = \begin{bmatrix} -5.26-2K_1 & -2.286-2K_2 & 2K_i \\ 1 & 0 & 0 \\ 0 & 1.1431 & 0 \end{bmatrix} \begin{bmatrix} x_1 \\ x_2 \\ x_i \end{bmatrix} + \begin{bmatrix} 0 \\ 1 \end{bmatrix} r(t) \tag{77}$$

The next step is to find the eigenvalues of a matrix A_{CL}. Substituting A_{CL} into (55) yields

$$0 = \det \left(\begin{bmatrix} \lambda & 0 & 0 \\ 0 & \lambda & 0 \\ 0 & 0 & \lambda \end{bmatrix} - \begin{bmatrix} -5.26-2K_1 & -2.286-2K_2 & 2K_i \\ 1 & 0 & 0 \\ 0 & 1 & 0 \end{bmatrix} \right) \tag{78}$$

Simplifying (78) yields

$$0 = \det \left(\begin{bmatrix} \lambda+5.26+2K_1 & 2.286+2K_2 & -2K_i \\ -1 & \lambda & 0 \\ 0 & -1.1431 & \lambda \end{bmatrix} \right) \tag{79}$$

Simplifying (79) obtains the characteristic equation of the closed-loop system expressed as

$$0 = \lambda^3 + 5.26\lambda^2 + 2\lambda^2 K_1 + 2.286\lambda + 2\lambda K_2 - 2.2862K_i \tag{80}$$

To achieve a faster rise time, the desired poles -2, -6, and -8 are selected. The desired characteristic equation is expressed as

$$0 = \lambda^3 + 16\lambda^2 + 76\lambda + 96 \tag{81}$$

The values for K_1, K_2 and K_i are solved by equating the coefficients of the like terms of the closed loop and desired characteristic equations (80) and (81). The equated characteristic equations are expressed as

$$16 = 5.26 + 2K_1 \tag{82}$$

and

$$76 = 2.286 + 2K_2 \tag{83}$$

and

$$96 = -2.2862K_i \tag{84}$$

K_i is expressed as

$$K_i = -41.9915 \tag{85}$$

K is expressed as

$$K = \begin{bmatrix} 5.37 \\ 36.8569 \end{bmatrix} \tag{86}$$

Substituting **K** and K_i into (77) yields the state space model of the closed loop system

$$\begin{bmatrix} \dot{\theta} \\ \ddot{\theta} \\ \dot{\theta}_i \end{bmatrix} = \begin{bmatrix} -5.26 & -2.2862 & 0 \\ 1 & 0 & 0 \\ 0 & -1.1431 & 0 \end{bmatrix} \begin{bmatrix} \theta \\ \dot{\theta} \\ \theta_i \end{bmatrix} + \begin{bmatrix} 2 \\ 0 \\ 0 \end{bmatrix} r(t) \tag{87}$$

$$y(t) = \begin{bmatrix} 0 & 1.1431 & 0 \end{bmatrix} \begin{bmatrix} x \\ x_n \end{bmatrix} \tag{88}$$

3. Simulink simulation

Fig. 4 shows the Simulink block diagram of the DC motor controlled by the FSFB controller with integral control added. The gain K is multiplied by the states and the output is fed back into the control system to alter the response. The output is fed back through an integrator and multiplied by the gain K_i. The gain K_i decreases the steady-state error that is fed back into the system.
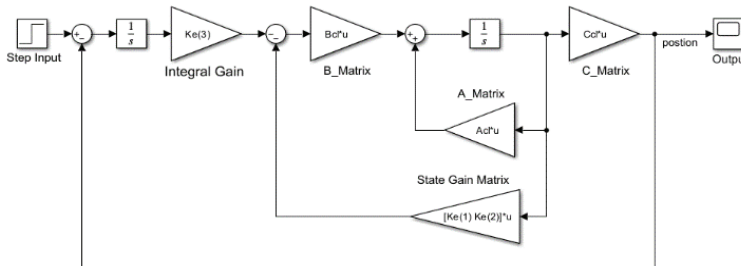

Fig. 4. DC Motor closed-loop control system FSFB and integral control

V. Case Study

Four cases are discussed and compared based on the different system responses and characteristics. The values for the matrices and the gains are input in the MATLAB environment and referenced in Simulink as variables. The models are tested using a step input and analyzed using the scope output function.

Case 1 describes the step response of the closed-loop DC motor system. Case 2 describes the step response of the closed-loop DC motor system with state feedback control. Case 3 and 4 describe the step response of the DC motor system with state feedback and integral control. The difference between cases 3 and 4 is the change in the input set point to compare the controller response to multiple inputs.

Fig. 5 to Fig. 8 show the step input responses for cases 1, 2, 3, and 4 respectively. In each case, the set point is compared to the angular position feedback of the DC motor. As shown, Case 1 has the slowest rise time as there is no addition of a controller to the system. Adding a FSFB controller causes Case 2 to have a faster rise time than Case 1, but the steady-state error is huge. The addition of integral control to the system reduces the steady state error to 0 which is seen in Case 3 and 4. The output graphs of the four cases are developed in MATLAB. The 'To-Workspace' function block is used to extract the positions and set points from Simulink to MATLAB to allow for custom plotting of the results as presented in Fig. 5 to Fig. 8.

Table II compares the rise time, settling time, steady-state error and overshoot percentage of the four test cases. According to the results, the characteristics of the closed-loop system are improved through controller design as clarified by the case studies. The results confirm that the FSFB controller with integral is the best controller for the required response of the DC motor. There is an increase in rise time when integral control is added, but a steady-state error of zero is achieved.
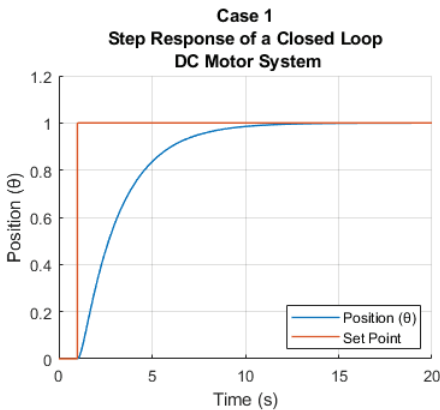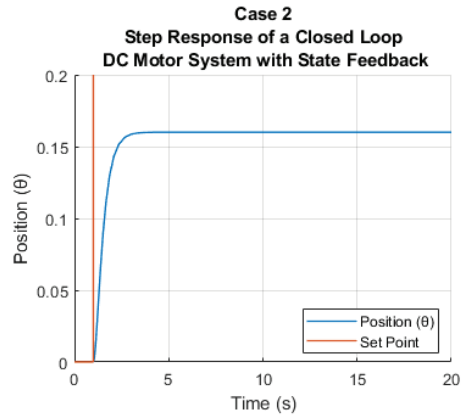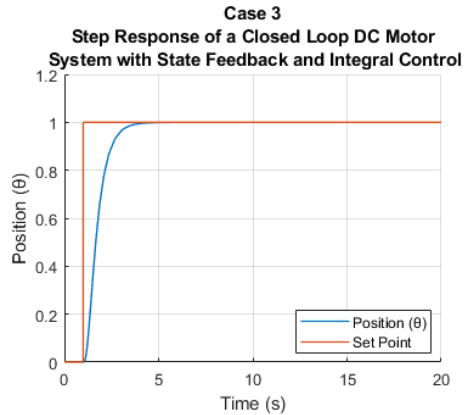

Fig. 6. Step response of system with FSFB control to an angular positional set point of 1

Fig. 7. Step response of system with FSFB and Integral Control to an angular positional set point of 1

Fig. 5. Step response of a closed loop DC motor System to an angular positional set point of 1
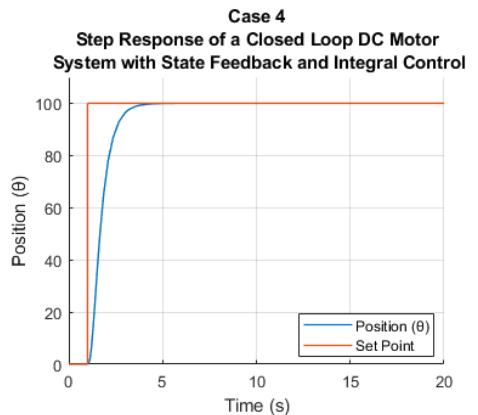

Fig. 8. Step response of system with FSFB and Integral Control to an angular positional set point of 100

TABLE II
COMPARISON BETWEEN DIFFERENT DC MOTOR CONTROLLERS

Case	Description	Step Input	Rise Time	Settling Time	Steady-state error
1	Closed loop system without a controller	1	4.013s	9.164s	0
2	Closed loop FSFB control	1	0.966s	2.714s	9.84
3	Closed loop FSFB with Integral control (Input = 1)	1	1.244s	3.303s	0
4	Closed loop FSFB with Integral control (Input = 100)	100	1.244s	3.303s	0

The closed loop system with FSFB and integral control is evaluated using a random number generator. This test aims to evaluate the closed loop system's capabilities of random setpoint tracking as well as to analyze the robustness and stability of the system. The output shown in Fig. 9 shows that the angular position consistently follows the random set points with the same response. The system is proven to also be stable when actuating the DC motor in the opposite direction as the response in Fig. 9 shows.
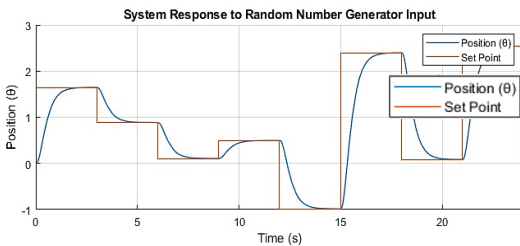

Fig. 9. Scope output of the FSFB controller with integral control response to a random number generator

VI. Conclusion

The electrical and mechanical components of a DC motor are found and combined to form the electro-mechanical mathematical model of the system. The Laplace transform is used to convert the model to the frequency domain to allow for easier algebraic manipulation of equations as well as easier conversion to Simulink block diagrams. Placeholder variables are used to further reduce the complexity of the model, which helps when converting to the state space equations. All calculations are provided to make it easier to adapt the mathematical model to any DC motor for testing purposes. Only the DC motor parameters are needed to use the calculation procedure outlined here.

The model is tested in four different cases. Firstly, a closed-loop system with encoder feedback without a controller is shown. In this case, the response of the system is very slow, and therefore a controller is needed. The addition of an FSFB controller reduced the rise time but increased the steady-state error. The controller is designed by converting the mathematical model to state space equations and then solving for the state matrix gain K which is used to alter the response of the system. The system response is simulated, and it is shown that the response is much faster, but the steady state error is huge.

Integral control is added to overcome the huge steady state error caused by the FSFB controller. The three controllers are simulated and compared, and the results showed that the full state feedback controller with integral control is the optimal controller to control the angular position of a DC motor.

Furthermore, the final control system is tested using a random input generator to test the system's set point tracking, robustness, and stability. The simulated results show that the control system can adapt to any change in set point at the same response rate each time.

The research contribution makes it easier to adapt the calculations to any DC motor as required. A means of testing the stability and robustness of the developed models is also provided. The future work will focus on the implementation of the system using a PLC environment and real-time implementation together with simulation.

VII. Conflict of Interest

The authors declare no conflict of interest in the publication process of the research article.

VIII. Author Contributions

Kevin Love conducted the research, drafted the paper, and analyzed the data; Nomzamo Tshemese-Mvandaba, reviewed, corrected, and edited the paper, and Carl Kriger reviewed and edited the paper; all authors approved the final version.

IX. References

[1] Maung, M. M. Latt, M. M. New, C. M. (2018) 'DC Motor Angular Position Control using PID Controller with Friction Compensation', International Journal of Scientific and Research Publications, 8(11), pp. 149-155. DOI: 10.29322/IJSRP.8.11. 2018. p8321.

[2] Aloo, L. (2016) 'DC Servomotor-based Antenna Positioning Control System using Hybrid PID-LQR Controller', European International Journal of Science and Technology, 5(2), pp. 17-31

[3] Eze, P. C. Ugoh, A. C. (2021) 'Positioning Control of DC Servomotor-Based Antenna Using PID Tuned Compensator', Journal of Engineering Sciences, 8(1), pp. E9-E16. DOI: 10.21272/jes.2021.8(1). e2

[4] Ma'arif, A. Setiawan, N. R. (2021) 'Control of DC Motor Using Integral State Feedback and Comparison with PID: Simulation and Arduino Implementation', Journal of Robotics and Control (JRC), 2(5), pp. 456-461. DOI: 10.181196/jrc.25122.

[5] Venugopal, K Manoharan, S. K. Megalingam, R. K. (2022) 'Position Estimation in DC Motor using Strain Gauge Closed Loop

Control for Robotic Grippers', 2022 IEEE IAS Global Conference on Emerging Technologies (GlobConET), pp. 355-360, DOI:10.1109/GlobConET53749.2022.9872356.

[6] Thein, M. M. Lwin, K. S. (2019) 'Implementation of DC Motor Controlling Techniques', International Journal of Science, Engineering and Technology Research (IJSETR), 8(7), pp. 345-251.

[7] Mezher, L. (2019) 'Position Control for Dynamic DC Motor with Robust PID Controller using MATLAB', International Journal of Advanced Trends in Computer Science and Engineering, 8(3), pp. 936-942. DOI: 10.30534/ijatcse/2019/92832019.

[8] Ye, N. N. Oo, K. Z. (2019) 'Design and Implementation of PID Controller for Motor Position Control', International Journal of Scientific & Engineering Research, 10(8), pp. 429-433.

[9] Saaf, M. (2021) 'Real Time DC Motor Position Control Using PID Controller in LabVIEW', Journal of Robotics and Control (JRC), 2(5), pp. 342-348, DOI:10.18196/jrc.25104.

[10] Rahman, N. N. A. Yahya, N. M. (2021) 'A mathematical model of a brushed DC motor system', Faculty of Manufacturing and Mechatronic Engineering Technology, College of Engineering Technology, 2(2), pp. 60-68, DOI: https://doi.org/10.15282/daam.v2i2.6830.

[11] Moulahcene, F. Laib, H. Merazga, A. (2022) 'Angular Position Control of DC Gear-Motor Using PID Controllers for Robotic Arm', International Conference on Electrical, Computer and Energy Technologies (ICECET 2022), pp. 1-6, DOI:10.1109/ICECET55527.2022.9872821.

[12] Flores-Moran, E. Yanez-Pazmino, W. Espin-Pazmino, L. (2022) 'Model Predictive Control and Genetic Algorithm PID for DC Motor Position', 2022 IEEE 40th Central America and Panama Convention (CONCAPAN), pp. 1-5, DOI:10.1109/CONCAPAN48024.2022.9997608.

[13] Moradi, S. Y. Saeedi, E. (2016) 'Controlling DC Motor Position, Using PID Controller Made by PIC Microcontroller', ZANCO Journal of Pure and Applied Sciences, p.p 29-36, DOI: 10.21271/zjpas.v28i2.807.

[14] Thamir, L. (2023) 'Performance of the Optimal Nonlinear PID Controller for Position Control of Antenna Azimuth Position System', International Information and Engineering Technology Association, 10(1), pp. 366-275. DOI: 10.18280/mmep.100143.

[15] Amini, S. Golpira, H. Bevrani, H. (2019) 'Robust H2 and H∞ Controller Design for DC Position Motor Control Under Uncertainties', The 6th International Conference of Control, Instrumentation, and Automation (ICCIA2019), pp. 1-6, DOI:10.1109/ICCIA49288.2019.9030972.

[16] Shafi, S. Hamid, P. S. Nahvi, S. A. (2023) 'Observer Based State Feedback Controller Design of a DC Servo Motor Using Identified Motor Model: An Experimental Study', 2023 International Conference on Power, Instrumentation, Energy and Control (PIECON), pp. 1-6, DOI:10.1109/PIECON56912.2023.10085764.

[17] Iswanto. Raharja, N. M. Ma'arif, A. Ramadhan, Y. Rosyady, P. A. (2021) 'Pole Placement Based State Feedback for DC Motor Position Control', Annual Conference on Science and Technology Research (ACOSTER) 2020. DOI: 10.1088/1742-6596/1783/1/012057.

[18] Pal, D. (2016) 'Modeling, Analysis and Design of a DC Motor based on State Space Approach', International Journal of Engineering Research & Technology (IJERT), 5(2), pp. 293-296. DOI: 10.17577/ijertv5is020332.

[19] Ahmad, M. Khan, A. Raza, M, A. Ullah, S. (2018). 'A Study of State Feedback controllers for Pole Placement', 5th International Multi-Topic ICT Conference (IMTIC). DOI: 10.1109/IMTIC.2018.8467276.

[20] Nur, A. A. Rahim, A. H. M. A. (2022) 'State feedback for DC Motor Position Control Based on Pole Position'.

[21] Ohemu, M. Onuche, A. D. F. Kachalla, I. A. Zuleihat, Z. K. (2022) 'State-feedback Control for a DC motor Using Pole Placement Technique', International Conference on Electrical Engineering Applications (ICEEA 2020).

[22] Sarkar, R. (2020) Basics of DC Motor. Available at: https://www.electronicsforu.com/resources/dc-motor-basics (Accessed: 18 April 2023).

[23] Rowell, D. (2002) 'State-Space Representation of LTI Systems', 2.14 Analysis and Design of Feedback Control Systems.